

PAPER

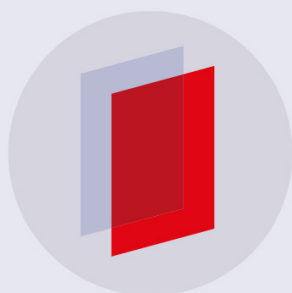
On the energy confinement time in spherical tokamaks: implications for the design of pilot plants and fusion reactors

To cite this article: P F Buxton *et al* 2019 *Plasma Phys. Control. Fusion* **61** 035006

View the [article online](#) for updates and enhancements.

Recent citations

- [On the confinement modeling of a high field spherical tokamak ST40](#)
A Yu Dnestrovskij *et al*



IOP | ebooks™

Bringing you innovative digital publishing with leading voices to create your essential collection of books in STEM research.

Start exploring the collection - download the first chapter of every title for free.

On the energy confinement time in spherical tokamaks: implications for the design of pilot plants and fusion reactors

P F Buxton , J W Connor, A E Costley, M P Gryaznevich and S McNamara

Tokamak Energy Ltd., 173 Brook Drive, Milton Park, Oxfordshire, OX14 4SD, United Kingdom

E-mail: peter.buxton@tokamakenergy.co.uk

Received 4 October 2018, revised 28 November 2018

Accepted for publication 11 December 2018

Published 22 January 2019



CrossMark

Abstract

Experiments on NSTX and MAST have shown the thermal energy confinement time in spherical tokamaks (STs), $\tau_{E,th}$, to have a stronger toroidal field and weaker plasma current dependence than in conventional large aspect ratio tokamaks. These scalings were derived for single machines both of which are similarly sized, consequently the NSTX and MAST scaling laws do not include a size dependence, and so cannot be used to extrapolate the performance of future STs. Using physics-based dimensional arguments we extend the NSTX scaling to include a size scaling. We also resolve a colinearity problem specific to NSTX data by assuming core transport is gyro-Bohm like. The resulting scaling has approximately zero beta dependence, a typical collisionality dependence, and a relatively weak safety factor dependence:

$B\tau_{E,th} \propto \rho_*^{-3} \nu_*^{-0.53} \beta^{-0.17} q^{-0.35}$. With the exception of the safety factor, all exponents are consistent with recent experiments in large aspect ratio tokamaks. This apparent difference between STs and large aspect ratio tokamaks is consistent with MAST and NSTX results. We have considered the implications of the scaling for pilot plants and reactors and find it may be possible to develop more compact reactors based on the ST approach.

Keywords: confinement time, spherical tokamaks, pilot plants and fusion reactors

(Some figures may appear in colour only in the online journal)

1. Introduction

Experimental scaling laws for thermal energy confinement time in large aspect ratio tokamaks are well established. They take the form $\tau_{E,th} \propto I_p^{\alpha_I} B_T^{\alpha_B} P_L^{\alpha_P} \bar{n}_e^{\alpha_n} R^{\alpha_R}$, where I_p is the plasma current, B_T the toroidal field at the plasma centre, P_L the loss power, \bar{n}_e the line averaged electron density, R the plasmas major radius. However, the confinement time database for spherical tokamak (ST) scaling is sparsely populated and essentially limited to one ‘size’ (MAST and NSTX), so α_R is undetermined. Analysis of the available ST databases displays rather unclear trends which are apparently different from those observed at large aspect ratio. These apparent differences have a significant effect on the predicted confinement of future STs, therefore it is sensible to develop a ST specific scaling law. In this paper we discuss the properties of the available ST scaling laws and how to exploit dimensional

analysis to extract the maximum amount of information from existing scalings, particularly the size dependence. Potential collinearities within the database limit the power of dimensional analysis and we also show how further generic theoretical ideas on the nature of local turbulent transport (Bohm or gyro-Bohm) can mitigate this. The scaling law including the size scaling is then applied to the design of an ignited ST device to ascertain the necessary size.

2. ST experimental energy confinement scaling laws

In 2006, experiments on NSTX [1] showed that the H-mode thermal energy confinement time, $\tau_{E,th}$, has a stronger dependence on the toroidal field and a weaker dependence on the plasma current than is predicted by the conventional large aspect ratio scaling IPB98(y, 2) [2] or the large aspect ratio,

Table 1. Comparison between different scaling laws. See equation (4) for the meaning of the dimensionless exponents x_{ρ_*} , x_{ν_*} , x_β and x_q . # indicates an exponent which has not been fitted. Italics indicates powers which have been derived by dimensional arguments (to derive α_R we use equation (6) and to derive the dimensionless exponents we use the transformations in table 2). It is important to note that if there are any underlying errors in the engineering exponents (for example due to correlations) these will propagate into the dimensionless physics variables; in particular we discuss correlations within the 2006 NSTX scaling in section 2.

	α_I	α_B	α_P	α_n	α_M	α_R	α_ϵ	α_κ	x_{ρ_*}	x_{ν_*}	x_β	x_q
NSTX2006, table 1 [1]	0.52	0.87	-0.50	0.27	#	2.63	#	#	-3.75	-0.45	-0.01	-0.59
NSTX2006, table 1 [1]	0.56	0.94	-0.40	0.00	#	2.81	#	#	-4.15	-0.54	0.33	-0.39
MAST2009, equation (2) [6]	0.51	1.60	-0.61	-0.06	#	3.70	#	#	-4.52	-0.77	1.11	0.45
MAST2011, equation (2) [9]	#	#	#	#	#	#	#	#	#	-0.82	#	-0.85
NSTX2013, figure 2 [7]	0.79	-0.15	#	#	#	#	#	#	#	#	#	#
NSTX2013, figure 5 [7]	#	#	#	#	#	#	#	#	-2.00	-1.50	#	#
NSTX2013, figure 5 [7]	#	#	#	#	#	#	#	#	-3.00	-1.90	#	#
IPB98(y, 2), equation (20) [2]	0.93	0.15	-0.69	0.41	0.19	1.97	0.58	0.78	-2.68	0.00	-0.90	-3.00
Petty2008, equation (36) [3]	0.75	0.30	-0.47	0.32	#	2.09	0.84	0.88	-3.00	-0.30	0.00	-1.12
McDonald, equation (40) [2]	0.72	0.09	-0.55	0.51	0.10	2.14	0.78	0.74	-2.77	-0.08	0.00	-1.56
Cordey, equation (10) [5]	0.85	0.17	-0.45	0.26	0.11	1.86	#	#	-2.80	-0.31	0.00	-1.24

beta-independent scalings by Petty [3], McDonald [4] and Cordey [5], see table 1. In 2009 this behaviour was also observed on MAST [6]. However, in 2013 experiments on NSTX with lithium evaporation [7] showed a reversal of this behaviour and a return to large aspect ratio like scaling. The difference between the 2013 NSTX result and the earlier NSTX and MAST results is thought to be due to differences in the wall conditions. Recently it has also been noted that the earlier NSTX and MAST scalings are more *typical* of ST confinement [8–10].

When the 2009 MAST scaling law is cast into dimensionless variables the scaling law shows: a stronger than gyro-Bohm dependence, a positive beta dependence and a strong size dependence, none of which are consistent with present experimental experience in conventional tokamaks or theoretical understanding. A possible reason for this discrepancy is correlations within the dataset, Valovič [6] found correlations both within dimensionless variables (ρ_* , β) and (β , q), and between the engineering variable: stored energy and toroidal field. Because of this, we choose to work with the 2006 NSTX confinement time scaling law.

Kaye noted that within the 2006 NSTX database there is a strong collinearity between P_L and \bar{n}_e [1]. The effect of this is that the database is poorly conditioned and it is difficult to distinguish between the effects of P_L and \bar{n}_e ; because of this the dimensionless scalings in table 1 are expected to be suspect. To mitigate this problem Kaye [1] used the principal component error-in-variable method which attempts to separate variables. To test how effective this was, Kaye produced two scalings, one including and the other excluding \bar{n}_e :

$$\tau_{E,\text{th}}^{\text{(NSTX including } \bar{n}_e)} = 0.091 I_p^{0.52} B_T^{0.87} \bar{n}_e^{0.27} P_L^{-0.5}, \quad (1)$$

$$\tau_{E,\text{th}}^{\text{(NSTX excluding } \bar{n}_e)} = 0.131 I_p^{0.56} B_T^{0.94} P_L^{-0.4}. \quad (2)$$

We note that the P_L exponent changes the most when \bar{n}_e was excluded, which is indicative of a correlation between the two predictors. However, we note that the I_p and B_T exponents also change, though to a lesser extent. Kaye also observed that the root mean square errors (RMSE) of both fits are

approximately equal: 0.158 including \bar{n}_e and 0.163 excluding \bar{n}_e . This indicates that both fits are equally valid, and suggests that the correlation has not been entirely removed.

By comparing the scalings we deduce that the correlation has the form:

$$\bar{n}_e^{\text{(correlation)}} = 3.3 P_L^{0.37}. \quad (3)$$

To directly probe the colinearity we have used data from the international global H-mode confinement database [11], and in figure 1 we show the correlation between \bar{n}_e and equation (3) (note, this is not the same database as was used to produce the scaling in [1]). The colinearity is clearly visible with relatively small scatter. The implication is that it is very difficult to separate the effects of density and power. As a consequence we have little confidence in the exact values of the α_n and α_P exponents.

3. Dimensional analysis and the size scaling

Before considering the NSTX data in detail we will present the key arguments that allow us to deduce a size scaling from data on a single machine by using dimensional arguments.

Assuming that transport is controlled by plasma physics and the plasma is quasi-neutral so that the Debye length does not play a role, then following Connor [12] and Kadomtsev [13], the confinement time scalings can be expressed as a power law fit in terms of dimensionless variables:

$$\tau_{E,\text{th},[\text{s}]}^{\text{(scaling)}} \propto \omega_{c_i}^{x_{\omega}} \rho_*^{x_{\rho_*}} \nu_*^{x_{\nu_*}} \beta^{x_\beta} A^{x_M} q^{x_q} \epsilon^{x_\epsilon} \kappa_a^{x_\kappa}, \quad (4)$$

where: $\omega_{c_i} \propto B_T A^{-1}$ is the cyclotron frequency; $\rho_* \propto A^{0.5} T^{0.5} \epsilon^{-1} R^{-1} B_T^{-1}$ is the normalised ion Larmor radius; $\nu_* \propto \bar{n}_e R T^{-2} q \epsilon^{-1.5}$ is the normalised collisionality; $\beta \propto \bar{n}_e T B_T^{-2}$ is the plasma beta; A is the mass of the main ion species normalised to the proton mass; $q \propto B_T R I_p^{-1} \epsilon^2 \kappa_a$ is the cylindrical safety factor; $\epsilon = a/R$ is the inverse aspect ratio; and $k_a = V_p/(2\pi^2 R a^2)$ is the effective elongation. By a substitution of these definitions into

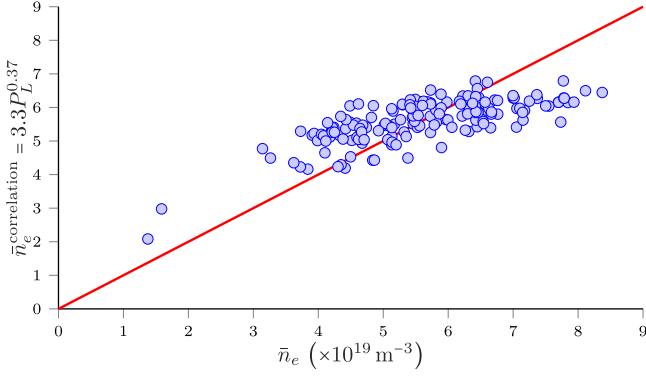


Figure 1. Shows the colinearity in NSTX between \bar{n} and P_L given in equation (3).

Table 2. Tables of transformations between scaling laws in engineering and dimensionless physics variables. This is a repeat of table 5 in [14], but with the collisionality defined as: $\nu_* \propto \bar{n}_e R T^{-2} q \epsilon^{-1.5}$ instead of $\nu_* \propto \bar{n}_e R T^{-2} q \epsilon^{-1}$.

$\tau_{E,\text{th}} \propto I_p^{\alpha_I} B_T^{\alpha_B} P_L^{\alpha_P} \bar{n}^{\alpha_n} A^{\alpha_M} R^{\alpha_R} \epsilon^{\alpha_\epsilon} \kappa_a^{\alpha_\kappa}$
$\tau_{E,\text{th}} \propto \omega_{ci}^{x_\omega} \rho_*^{x_\rho} \nu_*^{x_\nu} \beta^{x_\beta} M^{x_M} q^{x_q} \epsilon^{x_\epsilon} \kappa_a^{x_\kappa}$
<i>Engineering to dimensionless physics:</i>
$x_\omega = (\alpha_B + 0.2\alpha_I + 1.6\alpha_n - 0.4\alpha_P - 0.8\alpha_R)/(1 + \alpha_P)$
$x_{\rho_*} = (-1.2\alpha_I + 0.4\alpha_n - 3.6\alpha_P - 1.2\alpha_R)/(1 + \alpha_P)$
$x_{\nu_*} = (-0.2\alpha_I + 0.4\alpha_n - 0.6\alpha_P - 0.2\alpha_R)/(1 + \alpha_P)$
$x_\beta = (0.2\alpha_I + 0.6\alpha_n + 1.6\alpha_P + 0.2\alpha_R)/(1 + \alpha_P)$
$x_M = (\alpha_B + 0.8\alpha_I + \alpha_M + 1.4\alpha_n + 1.4\alpha_P - 0.2\alpha_R)/(1 + \alpha_P)$
$x_q = (-0.8\alpha_I - 0.4\alpha_n + 0.6\alpha_P + 0.2\alpha_R)/(1 + \alpha_P)$
$x_\epsilon = (\alpha_\epsilon + 0.5\alpha_I + \alpha_n - 2.5\alpha_P - 1.5\alpha_R)/(1 + \alpha_P)$
$x_\kappa = (\alpha_I + \alpha_\kappa + \alpha_P)/(1 + \alpha_P)$
<i>Dimensionless physics to engineering:</i>
$\alpha_I = (-x_{\nu_*} - x_q)/(1 - 0.5x_{\rho_*} + 2x_{\nu_*} - x_\beta)$
$\alpha_P = (0.5x_{\rho_*} - 2x_{\nu_*} + x_\beta)/(1 - 0.5x_{\rho_*} + 2x_{\nu_*} - x_\beta)$
$\alpha_M = (-x_{\omega_{ci}} + 0.5x_{\rho_*} + x_M)/(1 - 0.5x_{\rho_*} + 2x_{\nu_*} - x_\beta)$
$\alpha_\epsilon = (-2x_{\rho_*} + 4.5x_{\nu_*} - 2x_\beta + 2x_q + x_\epsilon)$
$\alpha_R = (-2.5x_{\rho_*} + 8x_{\nu_*} - 3x_\beta + x_q)/(1 - 0.5x_{\rho_*} + 2x_{\nu_*} - x_\beta)$
$\alpha_B = (x_{\omega_{ci}} - x_{\rho_*} + x_{\nu_*} - 2x_\beta + x_q)/(1 - 0.5x_{\rho_*} + 2x_{\nu_*} - x_\beta)$
$\alpha_n = (-0.5x_{\rho_*} + 3x_{\nu_*})/(1 - 0.5x_{\rho_*} + 2x_{\nu_*} - x_\beta)$
$\alpha_\kappa = (3x_{\nu_*} - 0.5x_{\rho_*} - x_\beta + x_q + x_\kappa)/(1 - 0.5x_{\rho_*} + 2x_{\nu_*} - x_\beta)$

equation (4) and noting that steady-state power balance requires: $P_L \propto \bar{n} T \epsilon^2 \kappa_a R^3 \tau_{E,\text{th}}^{-1}$, where P_L is the loss power, we can re-write $\tau_{E,\text{th}}^{(\text{scaling})}$ in engineering variables using the conversions listed in table 2. A similar procedure has been done by Luce [14], in which collisionality was defined as the electron collision frequency normalised by the toroidal transit time: $\nu_* \propto \bar{n}_e R T^{-2} q \epsilon^{-1}$. However, we take the same definition as in [2, 6, 9] and define collisionality as the effective collision frequency for detrapping normalised by the average bounce frequency, i.e. $\nu_* \propto \bar{n}_e R T^{-2} q \epsilon^{-1.5}$. Because of this

difference in definitions our transformations are slightly different.

If we suppose that the following engineering exponents have been found on a single machine:

$$\tau_{E,\text{th}} \propto I_p^{\alpha_I} B_T^{\alpha_B} P_L^{\alpha_P} \bar{n}^{\alpha_n} \quad (5)$$

then a size dependence can be deduced by requiring the scaling to be dimensionally correct (τ_E must have units of seconds). Considering the scaling in physics variables, we note that all of the variables are dimensionless except the cyclotron frequency which has units of inverse seconds. Therefore, for the scaling law to be dimensionally correct requires $x_\omega = -1$ (see table 2), solving for α_R we have:

$$\alpha_R = \frac{5}{4}\alpha_B + \frac{1}{4}\alpha_I + 2\alpha_n + \frac{3}{4}\alpha_P + \frac{5}{4}. \quad (6)$$

Using equation (6) we have deduced a size scaling for various single machine scaling laws in table 2.

However, if there is a strong correlation between engineering variables in the data set, then the scaling law (equation (5)) may be misleading, so that not all the exponents are well determined. In fact, if the dataset employed is not well-conditioned, such that there is a correlation, say

$$\bar{n}_e \propto P_L^y, \quad (7)$$

where y is a constant, then effectively there are only two independent exponents (α_I and α_B). The experimental scaling law from a single machine can then only be expressed as

$$\tau_E \propto B^{\alpha_B} I_p^{\alpha_I} P_L^{(\alpha_P + y\alpha_n)}. \quad (8)$$

The correlation, equation (7), prevents separate determination of the exponentials α_n and α_P , as there is now insufficient information to determine the size scaling. However, we do know the correlation variable y and the combined parameter ($\alpha_P + y\alpha_n$), which still contains some information about plasma confinement. This situation can be remedied if one makes a further physics-based assumption. The most robust assumption which we can make is to assume that local transport is either Bohm like ($x_{\rho_*} = -2$), gyro-Bohm like ($x_{\rho_*} = -3$) or somewhere between the two. Dedicated dimensionless experimental scans in large aspect ratio tokamaks [14] have shown the H-mode scaling to be gyro-Bohm. A comparison between experimental and theoretical work on NSTX has shown NSTX to be most consistent with gyro-Bohm scaling [15]. We shall therefore assume that transport is gyro-Bohm like.

Using the transformations listed in table 2 the exponents in equation (8) can be expressed in terms of dimensionless physics variables as:

$$\alpha_I = \frac{-x_{\nu_*} - x_q}{1 - 0.5x_{\rho_*} + 2x_{\nu_*} - x_\beta}, \quad (9)$$

$$\alpha_B = \frac{1 - x_{\rho_*} + x_{\nu_*} - 2x_\beta + x_q}{1 - 0.5x_{\rho_*} + 2x_{\nu_*} - x_\beta}, \quad (10)$$

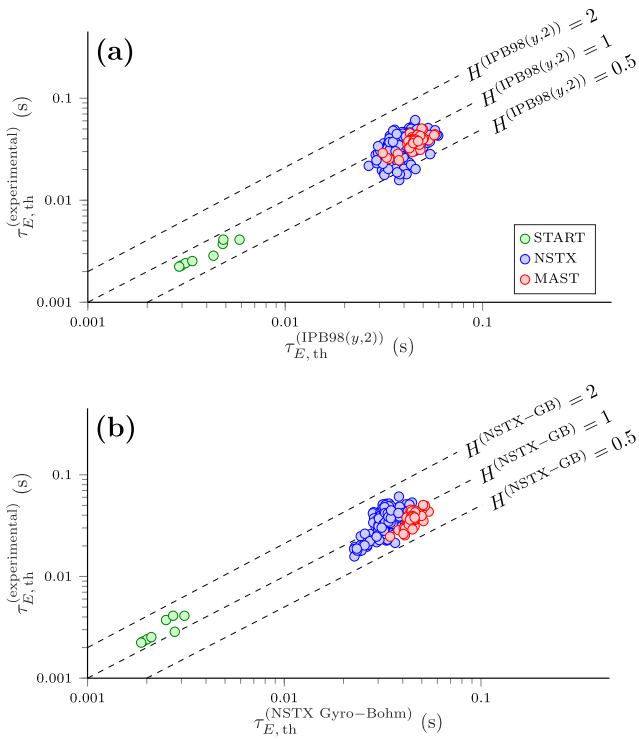


Figure 2. Comparison between (a) the IPB98($y, 2$) scaling and (b) the NSTX gyro-Bohm scaling (equation (13)) and experimental data in the DB4v5 database.

$$(\alpha_P + y\alpha_n) = \frac{0.5x_{\rho_*} - 2x_{\nu_*} + x_\beta}{1 - 0.5x_{\rho_*} + 2x_{\nu_*} - x_\beta} + y \left(\frac{-0.5x_{\rho_*} + 3x_{\nu_*}}{1 - 0.5x_{\rho_*} + 2x_{\nu_*} - x_\beta} \right). \quad (11)$$

Simultaneously solving equations (9)–(11), with $x_{\rho_*} = -3$ and knowing y and $(\alpha_P + y\alpha_n)$, allows us to find x_β , x_{ν_*} and x_q . Once these dimensionless coefficients have been found it is then straightforward to use the results in table 2 to transform into engineering variables.

4. New NSTX gyro-Bohm scaling law

Applying the procedure outlined in section 3 and simultaneously solving equations (9)–(11), with $x_{\rho_*} = -3$ (gyro-Bohm), $y = 0.37$ and $(\alpha_P + y\alpha_n) = -0.4$ for x_β , x_{ν_*} and x_q , we find that:

$$\tau_{E,th}^{(NSTX, \text{gyro-Bohm})} \propto \omega_{ci}^{-1} \rho_*^{-3} \nu_*^{-0.53} \beta^{-0.17} q^{-0.35} \quad (12)$$

which in engineering variables is:

$$\tau_{E,th}^{(NSTX, \text{gyro-Bohm})} = 0.21 I_p^{0.54} B_T^{0.91} P_L^{-0.38} \bar{n}_e^{-0.05} R^{2.14}. \quad (13)$$

We note that accounting for the colinearity has reduced both the density and power dependence (equation (13)); equation (1) and our result is very similar to Kaye's no density fit (equation (2)).

To test this new scaling we compare it to the experimental data from the low aspect ratio tokamaks START,

MAST and NSTX using the international global H-mode confinement database (ITPA database) [11]. Figure 2 shows a comparison between (a) the IPB98($y, 2$) scaling and (b) the new NSTX gyro-Bohm scaling (equation (13)); also included are the $H = 0.5$, $H = 1$ and $H = 2$ lines. Qualitatively we observe that the IPB98($y, 2$) scaling has a larger scatter and underpredicts the confinement. To compare these two scalings quantitatively, we calculate the RMSE. Treating each shot equally, the IPB98($y, 2$) scaling has RMSE = 0.27 and the NSTX gyro-Bohm scaling has RMSE = 0.20. Within the database there are 9 START shots, 252 NSTX shots, and 47 MAST shots, so the RMSE is skewed towards NSTX. If we discount START and weight MAST and NSTX equally, we find the IPB98($y, 2$) scaling has RMSE = 0.28 and the NSTX gyro-Bohm scaling has RMSE = 0.24.

Finally, we tested the sensitivity of this work to the assumption of gyro-Bohm transport. Comparing to the experimental data we find the gyro-Bohm scaling to be the best fit. In engineering dimensions the Bohm scaling has odd features (e.g. strong negative density dependence, $x_n = -0.62$), so we again discount the Bohm scaling. In section 6 we discuss the implications of the NSTX gyro-Bohm scaling, and have found that if we were to assume that transport is between Bohm and gyro-Bohm, ($x_{\rho_*} = -2.5$), then in the parameter range we are interested in there is only a small difference compared to the gyro-Bohm scaling.

5. Discussion of the NSTX gyro-Bohm scaling law

Several tokamaks have performed systematic scans of the dimensionless physics variables to try and determine how confinement dependence on the dimensionless variables. We note that many of these experiments were performed on conventional large aspect ratio tokamaks, so we are cautious of drawing too many conclusions for the low aspect ratio ST scaling, but the comparison is still interesting.

5.1. Beta dependence

Our analysis yielded $x_\beta = -0.17$. Previous beta scans have shown beta to have either a detrimental or no effect on confinement. In particular DIII-D and JET-C (i.e. with a carbon wall) found that confinement is unaffected by beta (JET-C found: $x_\beta = 0.01 \pm 0.11$), whereas JT-60U and ASDEX upgrade found increasing beta had a detrimental effect on confinement. More recently, experiments on JET-ILW (i.e. with an ITER like wall) may have resolved this apparent discrepancy by performing a beta scan at both high and low collisionality: at high collisionality, beta has a detrimental impact on confinement, whereas at low collisionality (where one wants to extrapolate towards) confinement is unaffected by beta [16, 17]. In table 1 we infer a beta dependence for MAST (by requiring the scaling to be dimensionally correct), however this result appears anomalous as the power is positive, $x_\beta = 1.11$. Having a weak or no beta dependence is an indication that the underlying core turbulence is dominated by electrostatic effects. Gyrokinetic modelling of MAST

discharges [10] showed that the underlying core turbulence is almost entirely electrostatic.

5.2. Collisionality dependence

Our analysis yielded $x_{\nu_*} = -0.53$. Scans on C-Mod, DIII-D, JET, JT-60U and Compass have found x_{ν_*} to have a range between -0.2 and -0.75 [14], with our result in the middle of this range. JET's metal ILW reported a dependence $x_{\nu_*} = -0.6$ which is in good agreement with our result, however, this result differs from that with the JET-C wall, $x_{\nu_*} = -0.33$ [16–18]. Unsurprisingly, our result is close to the collisionality dependence reported by the 2006 NSTX result, $x_{\nu_*} = -0.45$ [1], which our analysis is based on. This result is significantly weaker than the dependence reported on MAST, $x_{\nu_*} = -0.82$ [9]. Experiments on NSTX with lithium showed an increasingly strong dependence as collisionality decreases, at lower values of collisionality x_{ν_*} is between -0.79 and -1.21 [7].

5.3. Safety factor dependence

Our analysis yielded $x_q = -0.35$. This is closer to the MAST result: $x_q \approx -0.85 \pm 0.2$ [6, 9], than to results from DIII-D, which found the scaling of q_{95} to be $x_{q_{95}} = -1.43 \pm 0.23$ [14, 19], and most large aspect ratio scalings (see table 1). This difference appears to indicate a difference between conventional large aspect ratio and low aspect ratio tokmaks.

5.4. Power dependence

Our analysis yielded $\alpha_P = -0.38$. This dependence is weaker than the IPB98(y, 2) scaling, but more consistent with other beta-independent scaling laws, shown in table 1.

5.5. Density dependence

Our analysis yielded $\alpha_n = -0.05$. This dependence is weaker than is typical for most large aspect ratio tokmaks which is in the range 0.26 – 0.51 , but this result is in agreement with results from MAST: $\alpha_n = -0.06$ [6].

5.6. Size dependence

Our analysis yielded $\alpha_R = 2.14$. This result, the principle objective of our analysis, is in agreement with the majority of H-mode scalings, shown in table 1.

6. Implications for the size and power of ignited STs

To assess the implications of this new energy confinement scaling we use the tokamak energy system code [20, 21] and, as an idealised example, we consider the conditions necessary for ignition ($Q_{\text{fus}} = \infty$; 100% bootstrap) in a 2 m major radius ST ($R_{\text{Geo}} = 2$ m), assuming the NSTX gyro-Bohm scaling (equation (13)) with $H^{(\text{NSTX, gyro-Bohm})} = 1$. In practice we would not operate at ignition with 100% bootstrap; instead one would operate at a high fusion gain, in order to control the tokamak plasma.

To perform the conceptual study we held the following parameters constant: geometry ($R_{\text{Geo}}/a = 1.8$, elongation $\kappa = 3$, triangularity $\delta = 0.5$); $Z_{\text{eff}} = 1.6$; $P_T = 1.1$ (peaked temperature, where $T(r) = T_0(1 - (r/a)^2)^{P_T}$); $P_n = 0.7$ (flat density); alpha ash confinement $\tau_{\alpha}/\tau_{E,\text{th}} = 5$; normalised internal inductance $l_i(2) = 0.5$; and chose the lower temperature solution when more than one solution existed. When compared to NSTX the effective elongation is larger, and in all large aspect ratio scalings confinement time scales positively with elongation (see table 1), so we have most likely slightly under-predicted the confinement time. The reason we have chosen to operate with a high elongation is to drive bootstrap current more easily, which makes ignition easier. This value for the elongation is very similar to the proposed elongation in other concept studies for high performance STs, for example the ST fusion nuclear science facility [22], the component test facility [23], and the ST power plant [24]. Figure 3 shows the required magnetic field, plasma current, central temperature and fusion power required for ignition as a function of the normalised plasma beta (β_N) and the central electron density (n_{e0}). When no solution exists the plot is white. The low density interface between where a solution exists and where no solution exists corresponds to there being only one temperature solution. When we repeated this procedure using the IPB98(y, 2) scaling we found no ignited solutions with $H^{(\text{IPB98}(y,2))} = 1$.

Considering figure 3 we note that the most attractive operating points have central plasma temperatures between 16 and 20 keV which corresponds to a minimum in the toroidal field for a given fusion power. These low fusion power points are what we consider to be the most promising operating point from an engineering perspective, whilst meeting the objectives of high fusion gain. Following a contour of constant temperature, for example $T_0 = 18$ keV, as β_N increases so the fusion power increases and the required toroidal field decreases. This presents an interesting design optimisation problem where the optimal operating point must balance the divertor heat flux load and the neutron heating of the central post (which in a compact ST is significant [25, 26]) against the required magnetic field which places a higher demand on the engineering of the central column (maximum field on conductor and stresses). We have indicated an operating point (by a cross) which looks worthy of further, more detailed investigation; the parameters of this point are: $B_T = 4$ T, $I_p = 9.5$ MA, $P_{\text{fus}} = 350$ MW, $T_0 = 18$ keV, $n_{e0} = 2.3 \times 10^{20} \text{ m}^{-3}$, $\beta_N = 3.7$, $\bar{n}_e/n_{\text{GW}} = 0.78$ and $P_L/R_{\text{Geo}} = 21 \text{ MW m}^{-1}$. All of these appear plausible from an engineering perspective [27], but to fully verify this will require much more detailed investigation, in particular concerning the divertor and toroidal field coil. We note, that compared to the large aspect ratio scalings this operating point has high H -factors: $H^{(\text{IPB98}(y,2))} = 2.6$ and $H^{(\text{Petty}^{2008})} = 1.8$.

We have also considered the implications of this new scaling law for ST pilot plants, $Q_{\text{fus}} = 5$, holding the same geometric and plasma parameters constant as we did when considering the ignited ST, but reducing the size to $R_{\text{Geo}} = 1.5$ m. Qualitatively we find a similar operating

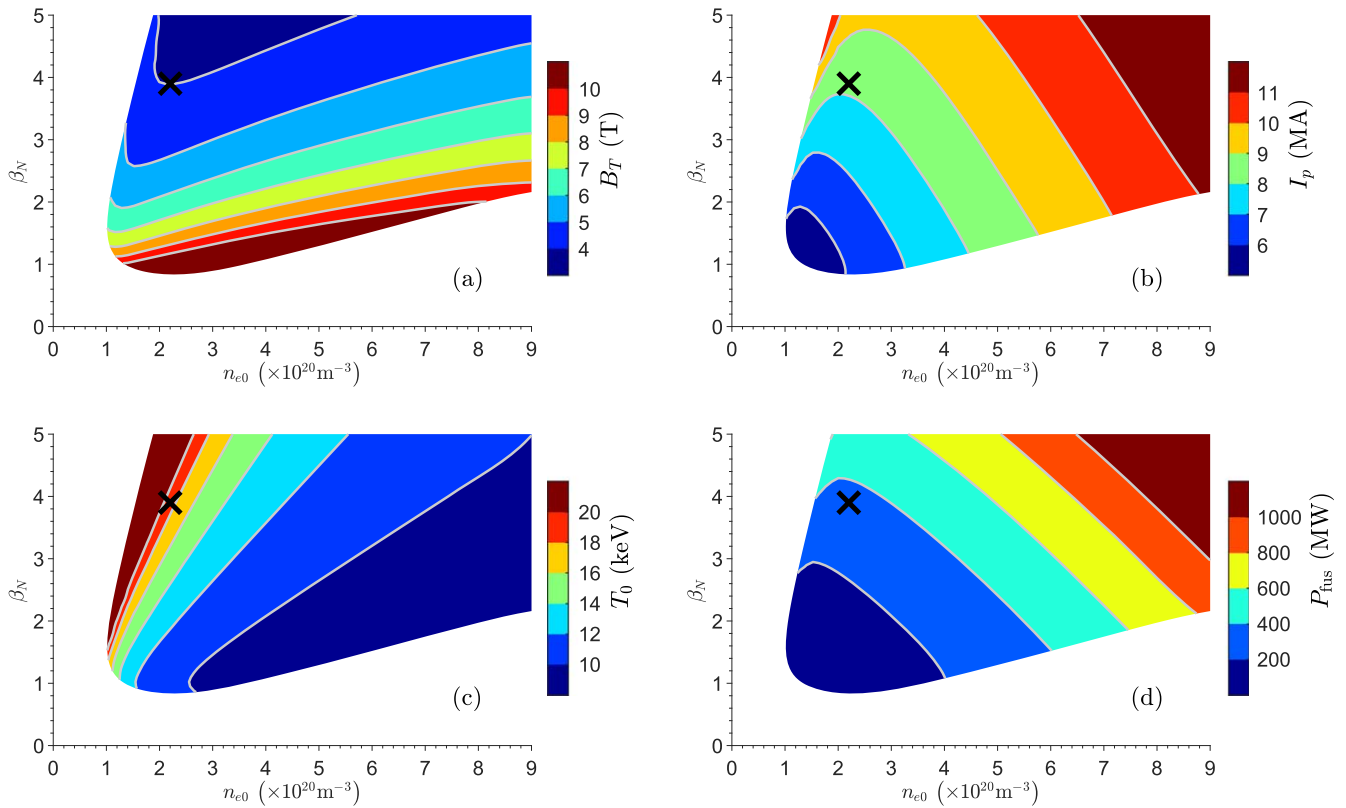


Figure 3. Shows the range of parameters where the conditions for ignition are met in a $R_{\text{Geo}} = 2$ m ST assuming that confinement follows the NSTX gyro-Bohm scaling (equation (13)) with $H = 1$. (a) Magnetic field; (b) plasma current; (c) central temperature; (d) fusion power, as a function of the normalised plasma beta (β_N) and central electron density (n_{e0}). We have indicated an operating point, with a cross, which we believe is worth further more detailed investigation. The following parameters are held constant: $R_{\text{Geo}}/a = 2/1.11 = 1.8$, $\kappa = 3$, $\delta = 0.5$, $Z_{\text{eff}} = 1.6$, $P_T = 1.1$, $P_n = 0.7$, $\tau_\alpha/\tau_{E,\text{th}} = 5$, $l_i(2) = 0.5$.

diagram to figure 6: where the optimum solutions have central plasma temperatures between 16 and 20 keV and again magnetic field and fusion power can be traded against each other. A potential operating point which appears plausible from an engineering perspective has the following parameters: $B_T = 3.8$ T, $I_p = 8.2$ MA, $P_{\text{fus}} = 180$ MW, $T_0 = 15$ keV, $n_{e0} = 1.8 \times 10^{20} \text{ m}^{-3}$, $\beta_N = 2.8$, $\bar{n}_e/n_{\text{GW}} = 0.71$ and $P_L/R_{\text{Geo}} = 23 \text{ MW m}^{-1}$. Compared to the large aspect ratio scalings this operating point has H -factors of: $H^{(\text{IPB98}(y,2))} = 1.9$ and $H^{(\text{Petty2008})} = 1.3$.

7. Summary and conclusions

Ideally, the thermal energy confinement time database would be large, well conditioned and contain data from several differently sized STs. This would allow a direct probing of the underlying physics. However, given that such a large well conditioned database does not exist, we have shown how simple dimensional arguments can be applied to glean as much information from the database as possible.

By assuming that transport is gyro-Bohm like and taking account of the colinearity within the NSTX dataset, we derived a new ST scaling for $\tau_{E,\text{th}}$, which now includes a size dependence. Of course, we cannot glean any information on geometrical dependencies, such as aspect ratio R_{Geo}/a or

effective elongation κ_a , from simple dimensional arguments alone. Therefore the scaling law we present is only valid when applied to tokamaks with similar geometry (aspect ratio, elongation, triangularity) as NSTX. We find the most notable difference between the scaling of $\tau_{E,\text{th}}$ in low aspect ratio versus conventional large aspect ratio tokamaks is the weak dependence on the safety factor.

It is important to note that recent work on NSTX with lithium appears to show that as collisionality decreases, so the dependence on collisionality increases in a beneficial manner. However, we have only considered the implications for the scaling which we have derived; in particular, we have considered what conditions would be necessary to achieve ignition in a $R_{\text{Geo}} = 2$ m ST, and found that these might be possible from an engineering perspective. We also note that if confinement follows the IPB98(y, 2) scaling then there is no ignited solution within a $R_{\text{Geo}} = 2$ m ST regardless of engineering considerations. We also find an engineeringly plausible ST pilot plant ($Q_{\text{fus}} = 5$) at the $R_{\text{Geo}} = 1.5$ m scale. It is worth noting that as size and Q_{fus} increase so the NSTX gyro-Bohm scaling predictions diverge from the large aspect ratio predictions in a favourable direction. Therefore, the apparently different confinement properties of STs potentially present a viable route to fusion power, and if confinement does indeed improve at lower collisionality it may be possible to have an even more compact ignited ST.

ORCID iDsP F Buxton  <https://orcid.org/0000-0002-0349-0434>**References**

- [1] Kaye S M, Bell M G, Bell R E, Fredrickson E D, LeBlanc B P, Lee K C, Lynch S and Sabbagh S A 2006 Energy confinement scaling in the low aspect ratio national spherical torus experiment (NSTX) *Nucl. Fusion* **46** 848
- [2] ITER Physics Expert Group on Confinement and Transport/ITER Physics Basis Editors 1999 Chapter 2: Plasma confinement and transport *Nucl. Fusion* **39** 2175
- [3] Petty C C 2008 Sizing up plasmas using dimensionless parameters *Phys. Plasmas* **15** 781
- [4] McDonald D C *et al* 2004 The beta scaling of energy confinement in ELMy H-modes in JET *Plasma Phys. Control. Fusion* **46** A215
- [5] Cordey J G *et al* 2005 Scaling of the energy confinement time with β and collisionality approaching ITER conditions *Nucl. Fusion* **45** 1078
- [6] Valovič M *et al* 2009 Scaling of H-mode energy confinement with I_p and BT in the MAST spherical tokamak *Nucl. Fusion* **49** 075016
- [7] Kaye S M, Gerhardt S, Guttenfelder W, Maingi R, Bell R E, Diallo A, LeBlanc B P and Podesta M 2013 The dependence of H-mode energy confinement and transport on collisionality in NSTX *Nucl. Fusion* **53** 063005
- [8] Kurskiev G S *et al* 2017 Scaling of energy confinement time in the globus-M spherical tokamak *Plasma Phys. Control. Fusion* **59** 045010
- [9] Valovič M *et al* 2011 Collisionality and safety factor scalings of H-mode energy transport in the MAST spherical tokamak *Nucl. Fusion* **51** 073045
- [10] Roach C M *et al* 2009 Gyrokinetic simulations of spherical tokamaks *Plasma Phys. Control. Fusion* **51** 124020
- [11] Thomsen K 2002 H-mode Database Working Group *et al*. The international global H-mode confinement database: storage and distribution *Fusion Eng. Des.* **60** 347–52
- [12] Connor J W and Taylor J B 1977 Scaling laws for plasma confinement *Nucl. Fusion* **17** 1047
- [13] Kadomtsev B B 1975 *Fiz. Plazmy* **1** 710 (in Russian)
- [14] Kadomtsev B B 1975 *J. Plasma Phys.* **1** 389
- [15] Luce T C, Petty C C and Cordey J G 2008 Application of dimensionless parameter scaling techniques to the design and interpretation of magnetic fusion experiments *Plasma Phys. Control. Fusion* **50** 043001
- [16] Frassinetti L *et al* 2016 Dimensionless scalings of confinement, heat transport and pedestal stability in JET-ILW and comparison with JET-C *Plasma Phys. Control. Fusion* **59** 014014
- [17] Litaudon X *et al* 2017 Overview of the JET results in support to ITER *Nucl. Fusion* **57** 102001
- [18] Frassinetti L *et al* 2016 Global and pedestal confinement and pedestal structure in dimensionless collisionality scans of low-triangularity H-mode plasmas in JET-ILW *Nucl. Fusion* **57** 016012
- [19] Petty C C *et al* 1998 Experimental constraints on transport from dimensionless parameter scaling studies *Phys. Plasmas* **5** 1695–702
- [20] Costley A E, Hugill J and Buxton P F 2015 On the power and size of tokamak fusion pilot plants and reactors *Nucl. Fusion* **55** 033001
- [21] Costley A E 2016 On the fusion triple product and fusion power gain of tokamak pilot plants and reactors *Nucl. Fusion* **56** 066003
- [22] Menard J *et al* 2016 Fusion nuclear science facilities and pilot plants based on the spherical tokamak *Nucl. Fusion* **56** 106023
- [23] Peng Y M *et al* 2005 A component test facility based on the spherical tokamak *Plasma Phys. Control. Fusion* **47** B263
- [24] Voss G, Bond A, Hicks J and Wilson H 2002 Development of the spherical tokamak power plant *Fusion Eng. Des.* **63** 65–71
- [25] Windsor C G, Morgan J G and Buxton P F 2015 Heat deposition into the superconducting central column of a spherical tokamak fusion plant *Nucl. Fusion* **55** 023014
- [26] Windsor C G, Morgan J G, Buxton P F, Costley A E, Smith G W and Sykes A 2016 Modelling the power deposition into a spherical tokamak fusion power plant *Nucl. Fusion* **57** 036001
- [27] Sykes A *et al* 2017 Compact fusion energy based on the spherical tokamak *Nucl. Fusion* **58** 016039